

11B.5 PREDICTION AND MITIGATION OF ANOMALOUS PROPAGATION

James J. Stagliano*, J. Clayton Kerce, Bonnie Valant-Spaight

Propagation Research Associates, Inc.

1. INTRODUCTION

Anomalous propagation (AP) impacts the quality of precipitation estimates and many decisions, public safety resource management, and economic, that rely on accurate geolocated precipitation measurements. Techniques to automatically identify and mitigate the effects of AP in the radar data have been developed and implemented in systems such as the Hydrological Decision Support System (HDSS) and the Radar Echo Classifier (REC). These techniques detect AP through its statistical properties in the radar data and remove contaminated data.

Stagliano (2008) described a process to forecast and mitigate anomalous propagation through modeling the propagation environment. Sounding data is ingested into WRF which produces a three dimensional refractivity field. The refractivity field is ingested into propagation modeling software which modeled the propagation environment. The forecast element developed naturally from WRF forecasting the future conditions.

The process performed reasonably well provided the soundings were of sufficient resolution to capture the phenomena producing the AP. As discussed in Stagliano (2008), there are cases where the first data point of a sounding is above the inversion layer causing the AP. In these cases, WRF fails to capture the conditions resulting in AP.

The process described herein extends that earlier work by preparing a propagation module for WRF to directly model the propagation environment. The propagation model is being developed with consideration of adjoint development allowing WRF to assimilate radar data to discipline the model with respect to the measured propagation environment.

This paper briefly reviews anomalous propagation, briefly describes the model under development, and applies the model to a significant AP event around Wilmington, NC on June 7, 2008.

2. PHENOMENOLOGY

2.1. ANOMALOUS PROPAGATION REVIEW

Anomalous propagation, also known as range clutter, occurs when the radar beam is bent down to the earth's surface. This phenomenon results from atmospheric refractivity gradients.

If the atmosphere was homogenous electromagnetic radiation would travel in a straight line. However, the atmosphere is not homogeneous, rather it is stratified, thus the index of refraction, n , varies with altitude. For this review, we will use the standard assumption of horizontal homogeneity, though this assumption

is not true in general. Thus, the index of refraction can be considered as layered within the atmosphere as shown in Figure 1. Though the index of refraction varies, its variation is quite small. Therefore, it is standard to transform the index of refraction n into *refractivity* units, N via the definition,

$$N = (n - 1) \times 10^6 \quad (1)$$

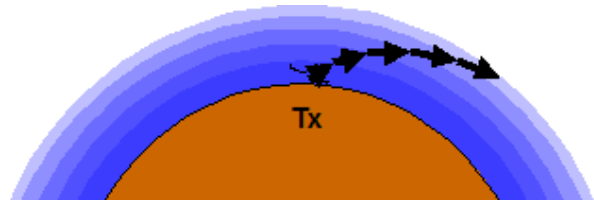


Figure 1 The stratified index of refraction due to the nonhomogeneous atmosphere.

For example, the index of refraction for air at standard temperature, pressure, and humidity is accepted to be $n_{air} = 1.000298$, its refractivity is $N_{air} = 298$ N-units.

The associated vertical gradient of refractivity with respect to index of refraction is,

$$\frac{dN}{dh} = \frac{dn}{dh} \times 10^6 \quad (2)$$

Thus, the variation in refractivity is proportional to the variation in the index of refraction.

Consider a radar scanning at an elevation ϕ . As the ray travels outward through the different layers, it is bent a little as it traverses from one layer to the next. The amount of bending is described by the *curvature*, the change in angle with respect to arclength,

$$C(h) = \frac{d\phi}{ds} = \frac{dn}{dh} \quad (3)$$

The curvature of the ray *with respect to the surface of the Earth* is given by adding this curvature to the reciprocal of the radius of the Earth,

$$C_E(h) = \frac{1}{R_E} + \frac{dn}{dh} \quad (4)$$

As an example, consider a ray that follows the Earth curvature, i.e. the ray stays at a constant height above the surface of the earth. The curvature with respect to the earth surface is zero, $C_E(h) = 0$ resulting in vertical gradient in the index of

refraction of $\frac{dn}{dh} = -1.569 \times 10^{-4} \frac{1}{km}$, which gives the

*Corresponding author address: James. J. Stagliano, Propagation Research Associates, Inc., 1275 Kennestone Circle, Suite 100, Marietta, Ga 30066; e-mail: jim.stagliano@pra-corp.com

associated refractivity gradient of $\frac{dN}{dh} = -156.9 \frac{N-units}{km}$. Thus

when $\frac{dN}{dh} > -156.9 \frac{N-units}{km}$, the ray will bend away from the

Earth's surface and out towards space. Similarly, when the gradient is less than -157 N-units/km, the ray will bend towards the Earth's surface. The refractivity gradient is used to classify the refractive environment into three general types, subrefractive where there is significant bending away from the earth's surface, normal propagation, and superrefraction where the rays bend back towards the earth's surface. This classification is summarized in Table 1 (Battan, 1981) and Figure 2.

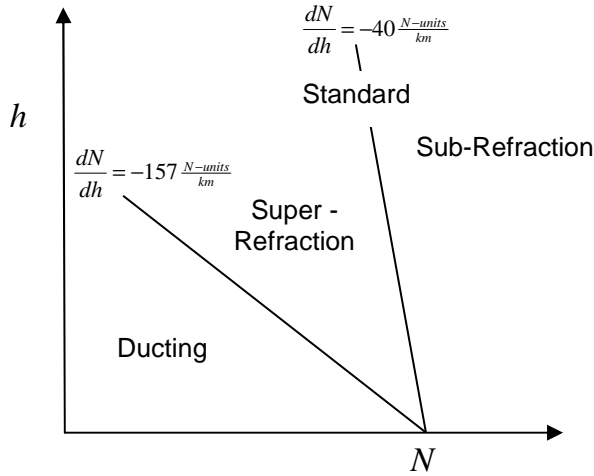


Figure 2 The refractive regimes

It is the latter classification, the ducting environment that causes AP.

A common exercise is to determine the curvature, or actually the reciprocal of the curvature (or effective Earth radius) that results in a straight line path for the electromagnetic pulse for a "standard" atmosphere. The vertical gradient for the standard atmosphere is

$\frac{dN}{dh} = -40 \frac{N-units}{km}$ (Battan, 1981), resulting in an effective Earth

radius of $R' = 1.34R_E \approx \frac{4}{3}R_E$. Thus, the standard assumption

of the 4/3 Earth radius comes from assuming a standard atmosphere. In reality, the effective Earth radius can vary from 1.1 R_E to 1.6 R_E based upon atmospheric conditions (Rinehart, 1991).

As the AP phenomenon is strongly dependent upon a highly negative gradient in the refractivity, it is natural to review the atmospheric conditions that result in these gradients.

2.2. Atmospheric Conditions associated with AP

The refractivity is dependent upon the atmospheric pressure, temperature, and partial water vapor pressure (Bean, 1966), via change in refractivity is thus,

Table 1 Refractive Environment Classification

Vertical Gradient of Refractivity	Refractive Environment
$\frac{dN}{dh} > 0 \frac{N-units}{km}$	Subrefractive
$0 > \frac{dN}{dh} > -156.9 \frac{N-units}{km}$	Super Refraction
$-157 \frac{N-units}{km} > \frac{dN}{dh}$	Ducting

$$N(p, T, e) = a \frac{p}{T} + b \frac{e}{T^2} \quad (5)$$

where $a = 77.6 \frac{K \cdot N-units}{mbar}$ and $b = 3.379 \times 10^5 \frac{K^2 \cdot N-units}{mbar}$. The

$$dN = \left(\frac{\partial N}{\partial p} \right) dp + \left(\frac{\partial N}{\partial T} \right) dT + \left(\frac{\partial N}{\partial e} \right) de \quad (6)$$

$$dN = \left(\frac{a}{T} \right) dp - \left(\frac{ap}{T^2} + \frac{2be}{T^3} \right) dT + \left(\frac{b}{T^2} \right) de \quad (7)$$

To understand the sensitivity of the refractivity to the variation in each variable, i.e. the weighting on the refractivity gradient by the atmospheric variables, consider the standard pressure and temperature at 50% relative humidity. In this case, $T = 293$ K, $p = 1013$ mbar, and $e = 23.4$ mbar. The differential refractivity is,

$$dN = 0.265dp - 1.61dT + 4.35de \quad (8)$$

The conditions that result in AP may be estimated for each variable by holding the others constant. Table 2 shows the results. The temperature and humidity gradients are physically realizable.

Table 2 AP Conditions in standard atmosphere

AP Criterion	Description
$\frac{dp}{dh} < -592 \frac{mbar}{km}$	A very sharp pressure decrease
$\frac{dT}{dh} > 97.5 \frac{K}{km}$	A sharp temperature increase
$\frac{de}{dh} < -36 \frac{mbar}{km}$	A significant decrease in water vapor partial pressure

Possibly the most probable atmospheric conditions resulting in AP is the latter one, a significant decrease in relative humidity with altitude. This occurs many times on clear nights when the air near the surface is quite moist and there is a sharp decrease in moisture content with height. This occurs when warm dry air moves over bodies of cool water

The next most likely event is a temperature inversion. In this scenario, the temperature sharply increases as a function of height, similar to that shown in Figure 3. This will occur on

clear nights where the ground cools more quickly than the air above it. Thus, temperature inversions occur quite often in the between late autumn and early spring.

The temperature increases from 10 deg C at about 50 m to about 6 deg C at 500 m at which point it increases again to approximately 13 deg C at 550 m. Thus the temperature inversion occurs between 500 and 600 m with a gradient of 140 K/km. Again, this gradient is sufficiently large to result in AP.

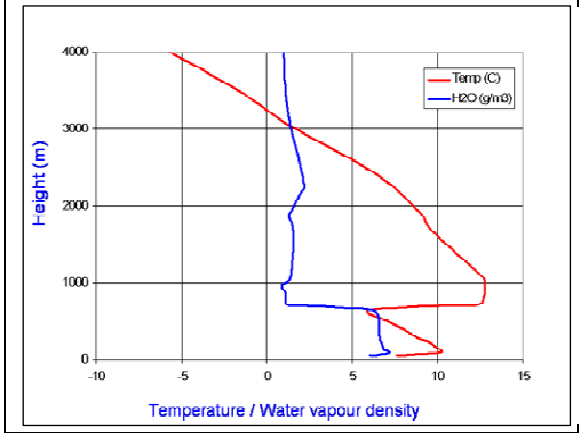


Figure 3 Profile showing temperature inversion. This profile was measured Nov. 7, 2006 over Herstmonceux UK

2.3. APPROACH

Stagliano (2008) discusses using atmospheric sensors (other than radar) to provide the initialization data for WRF. WRF subsequently estimates a three dimensional refractivity field in the future. The 3D refractivity field is fed into electromagnetic propagation modeling routines that estimate the propagation environment, determining if there is the presence of AP, where to expect the AP in the radar products and the antenna elevations needed to mitigate the AP. In that paper, Stagliano noted that the inversion layer resulting in AP around Atlanta was not being captured in the sounding data.

The lack of ability to capture the inversion resulting in AP is a significant impediment to any AP prediction and mitigation scheme. In this paper, a complementary tact is taken with a doubly pronged approach.

The first step in the approach is to use the available sensors profiling the atmosphere to discipline WRF. WRF will generate an initial refractivity field forecast. The radar becomes a sensor for input into WRF, allowing radar data (and hence any detected AP) to discipline the WRF data fields. From the 3D refractivity field, WRF will then generate the AP forecast.

To perform the assimilation of the radar data and produce the AP forecast, an electromagnetic (EM) propagation module is being developed for WRF. The currently available propagation models are very complicated to optimize the environment accuracy and processing resources. This added complexity results in an inability to adequately develop the adjoint model for data assimilation. The EM propagation model PRA is generating differs in that it is being developed with adjoint development in mind to assist in the assimilation of the radar data.

2.4. Propagation Modeling

The propagation modeling routine traces the projected rays from the radar site for a particular azimuth and elevation. The propagation modeling uses the standard Parabolic Equation Method (PEM).

PEM was developed in the 1940's for studies of radio waves within the atmosphere (Leontovich, 1946). Assuming azimuthal symmetry or alternatively the use of a very directional antenna, Maxwell's equations are reduced to the two dimensional scalar Helmholtz wave equation (Kuttler, 2002),

$$\nabla^2 \psi + k^2 n^2 \psi = 0, \quad (9)$$

where k is the wavenumber in free space, n is the refractive index, and ψ is the amplitude of the scalar field.

To approximate wide angle plane wave propagation in the troposphere, one can utilize the forward scattering approximation to Eqn. (9). Assuming that the depolarization due to atmospheric inhomogeneities is negligible results in the Claerhout approximation,

$$\left(1 + \frac{1}{4} \left\{ \frac{1}{k^2} \frac{\partial^2}{\partial z^2} + (n^2(z) - 1) \right\}\right) \frac{\partial \psi}{\partial x} = \frac{jk}{2} \left\{ \frac{1}{k^2} \frac{\partial^2}{\partial z^2} + (n^2(z) - 1) \right\} \psi(x, z), \quad (10)$$

with constant boundary conditions,

$$\begin{aligned} \psi(x_1, z) &= g(z) \\ \psi(x, z_1) &= 0 \\ \psi(x, z_N) &= 0 \end{aligned}, \quad (11)$$

Eqn. 10 is generally regarded to be valid up to 15 degrees away from the antenna pointing angle.

Simple boundary conditions are assumed and the function $g(z)$ is assumed to be Gaussian with characteristics consistent with a 3 dB antenna pattern beamwidth at a distance x_1 from the focal point,

$$g(z) \propto e^{-0.7 \lambda^2 / (\theta_{BW}^2 z^2)}. \quad (12)$$

Note, both θ_{BW} and x_1 are dependent on the antenna diameter and wavelength.

To develop the propagation model, Eqn. (10) needs to be discretized. This is performed by defining,

$$\begin{aligned} u_{p-1}^m &= \psi(x_m, z_p) \\ \tilde{u}_{p-1}^m &= \psi(\xi_m, z_p) \end{aligned}, \quad (13)$$

Obtaining second order accuracy to the numerical approximation is obtained by applying the following definitions

$$\frac{\partial \psi(\xi_m, z_p)}{\partial x} \approx \frac{u_p^{m+1} - u_p^m}{\Delta x} \quad (14)$$

$$\frac{\partial^2 \psi(x_m, z_p)}{\partial z^2} \approx \frac{u_{p+1}^m - 2u_p^m + u_{p-1}^m}{\Delta z^2} \quad (15)$$

$$\frac{\partial^2 \psi(\xi_m, z_p)}{\partial z^2} \approx \frac{\tilde{u}_{p+1}^m - 2\tilde{u}_p^m + \tilde{u}_{p-1}^m}{\Delta z^2} \quad (16)$$

$$\tilde{u}_p^m \approx \frac{u_p^{m+1} + u_p^m}{2} \quad (17)$$

$$\frac{\partial}{\partial z^2} \left(\frac{\partial \psi(x_m, z_p)}{\partial x} \right) \approx \frac{1}{\Delta x \Delta z^2} \left[(u_{p+1}^{m+1} - u_{p+1}^m) - 2(u_p^{m+1} - u_p^m) + (u_{p-1}^{m+1} - u_{p-1}^m) \right] \quad (18)$$

Substituting the approximations given by Eqns. (13)-(18) into Eqn. (10) results in a system of equations that can be represented in matrix form as,

$$\mathbf{A} \bar{u}^{m+1} = \mathbf{B} \bar{u}^m + \bar{c} \quad (19)$$

where the vector \bar{c} represents the boundary conditions and the matrices \mathbf{A} and \mathbf{B} are tridiagonal given by,

$$\mathbf{A} = \begin{bmatrix} a_{0,1} & 1 & 0 & \cdots & 0 \\ 1 & a_{0,2} & 1 & \ddots & \vdots \\ 0 & 1 & a_{0,3} & \ddots & 0 \\ \vdots & \ddots & \ddots & \ddots & 1 \\ 0 & \cdots & 0 & 1 & a_{0,p} \end{bmatrix} \quad (20)$$

and

$$\mathbf{B} = \begin{bmatrix} b_{0,1} & b_1 & 0 & \cdots & 0 \\ b_1 & b_{0,2} & b_1 & \ddots & \vdots \\ 0 & b_1 & a_{0,3} & \ddots & 0 \\ \vdots & \ddots & \ddots & \ddots & b_1 \\ 0 & \cdots & 0 & b_1 & b_{0,p} \end{bmatrix} \quad (21)$$

where

$$b_1 = \frac{1+jk}{1-jk}, \quad (22)$$

$$a_{0,p} = \alpha_p + \beta_p, \quad (23)$$

and

$$b_{0,p} = \alpha_p - \beta_p, \quad (24)$$

with the definitions,.

$$\gamma_p = n^2(z_p) - 1, \quad (25)$$

$$\alpha_p = \frac{[\gamma_p + 4]k^2 \frac{\Delta z^2}{\Delta x} - 2}{1-jk}, \quad (26)$$

$$\beta_p = \frac{2kj(1-k^2\Delta z^2\gamma_p)}{1-jk}. \quad (27)$$

Eqn. (19) can be solved using standard tridiagonal matrix techniques, however if the γ_p is real, the solution will show reflections from the upper boundary. This is mitigated by adding an imaginary term to γ_p to serve as a dampening mechanism.

3. RESULTS

This propagation modeling technique was applied to a significant AP event from June 7, 2008 at the Wilmington, NC WSR-88D site (KLTIX). Figure 4 shows the reflectivity product from a 0.5 deg elevation. The AP is obvious from 80m to 120 from the radar location. Figure 5 and Figure 6 show the associated reflectivity products from neighboring WSR-88D sites, KMHX and KCAE respectively. The former shows some AP while the latter the radar beam was above the AP.

It is interesting to note the nonhomogeneity in the AP observed from KTLX. The AP to the north of the radar is narrower and farther from the radar than that from the south. This indicates that the inversion layer to the north is higher and

thinner than in the south. This clearly shows a gradient in the inversion layer.

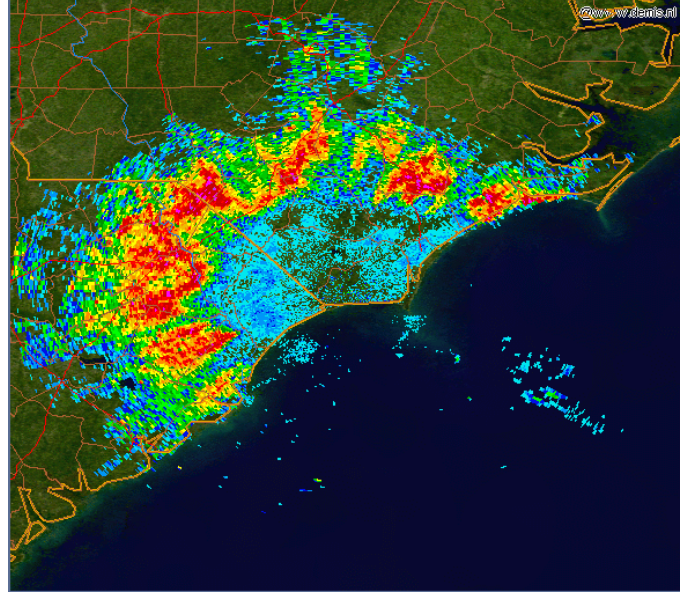


Figure 4 Base reflectivity from Wilmington, NC (KLTIX) June 7, 2008 at 12:43 UTC.

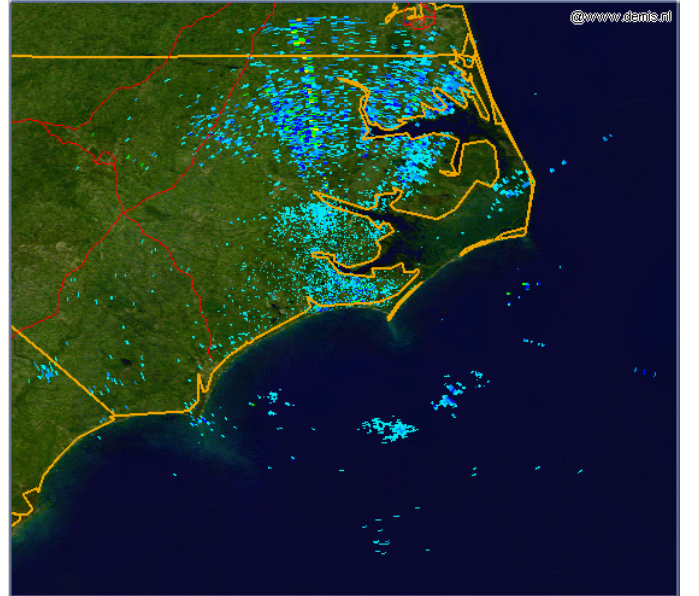


Figure 5 Base Reflectivity from Morehead City, NC (KMHX) June 7, 2008 at 12:43 UTC.

Figure 7 and Figure 8 show the associated soundings from Morehead City (MHX) and Charleston (CHS) and Figure 9 and Figure 10 are the respective vertical gradients. The sounding data confirms our assessment that the inversion layer at the North (MHX) is narrower and not as strong as that in the South (CHS).

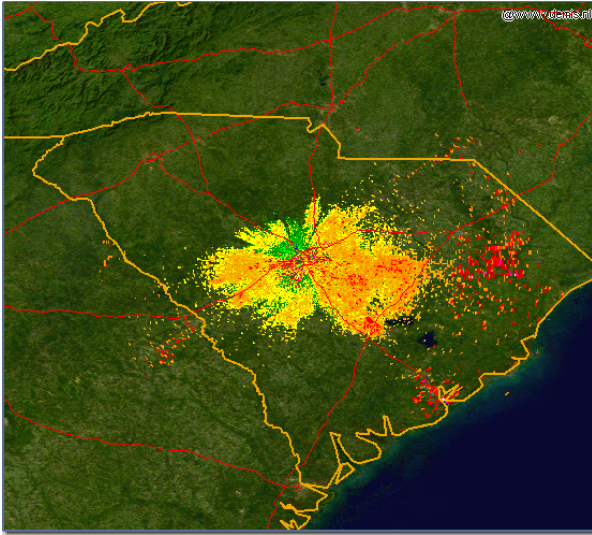


Figure 6 Base reflectivity from Columbia, SC (JCAE) June 7, 2008 at 12:43 UTC.

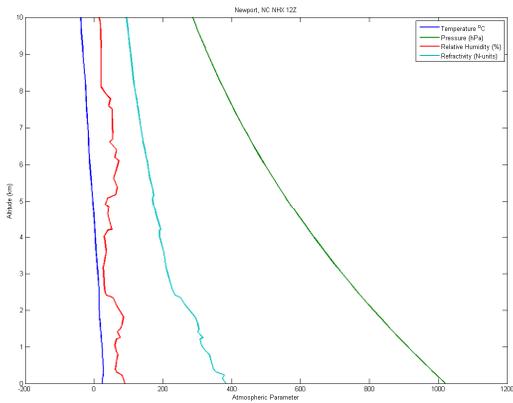


Figure 7 Atmospheric profile from Morehead City, NC (MHX) on June 7, 2008 at 12:00 UTC.

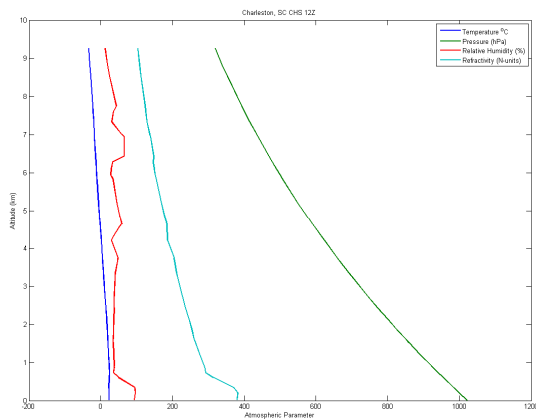


Figure 8 Atmospheric Profile from Charleston, SC (CHS) on June 7, 2008 at 1200 UTC

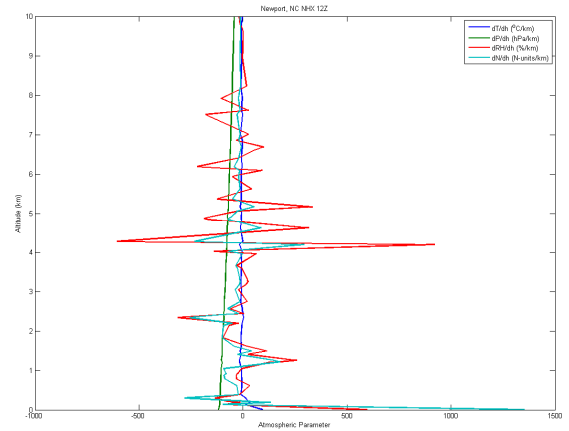


Figure 9 Vertical profile gradients from Morehead City, NC (MHX) on June 7, 2008 at 12:00 UTC

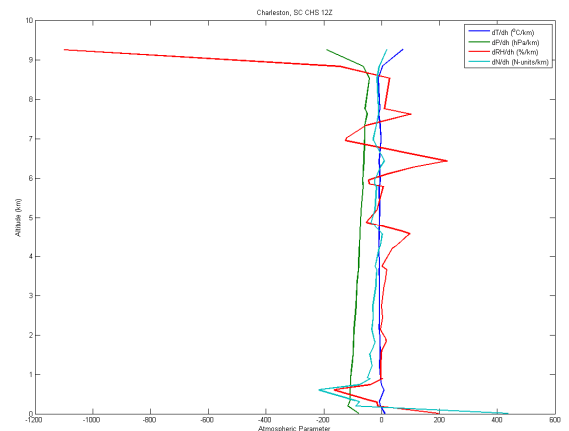


Figure 10 Vertical profile gradients from Charleston, SC (CHS) on June 7, 2008 at 12:00 UTC

Using these soundings, the propagation environment was simulated using Eqn. (10) with typical results shown in Figure 11. The simulation captured the AP characteristics with the ground reflection shown at approximately 80 km from the radar system, consistent with the results from WSR-88D.

A concern of the simulation is the step-size used to simulate the propagation environment. The step-size is a percentage of the wavelength being modeled. If we assume the step-size is 1/10 of the wavelength then for a S-band radar, there are 100,000 by 100,000 grid points per a km. Thus, the modeling environment is computationally intensive.

To optimize the simulation processing, the simulation was performed at different wavelengths to determine the minimum frequency which the propagation effects would be demonstrated qualitatively. Figure 12 shows the propagation environment around Wilmington, NC simulated with a wavelength of 40 cm, capturing the AP effects. The difference in computational requirements is significant with the CPU time of 170 seconds required for the 10 cm wavelength and 12 seconds for the 40 cm wavelength.

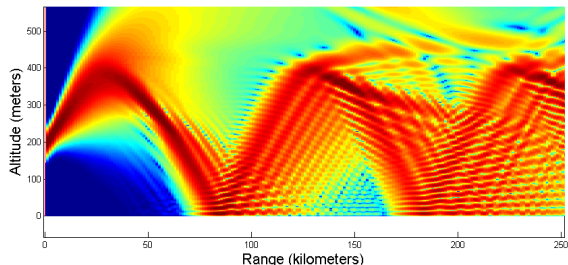


Figure 11 Results from the propagation environment simulation for Wilmington, NC on June 7, 2008 at 12:43 UTC.

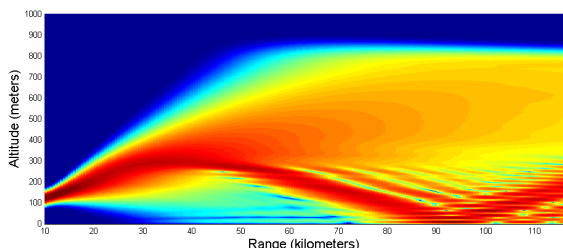


Figure 12 Results from the propagation environment simulation for Wilmington, NC on June 7, 2008 at 12:43 UTC using a wavelength of 40 cm.

4. CONCLUSION

In previous work, Stagliano et al. introduced the concept of using WRF to estimate the 3D refractive field which becomes input to a propagation environment modeling program. This seemed to work well *if* the local sounding captured the inversion layer. However, it was noted that at least in the Atlanta area, the first data point of the local sounding usually occurs *above* the inversion layer causing the AP behavior. Thus, to improve the propagation modeling, it would be advantageous to assimilate the radar data showing the AP. The ultimate goal of this work is to develop a WRF module that would perform the propagation environment modeling and the associated adjoint for assimilating the radar data..

The standard propagation modeling software have many complicated and hybrid propagation models whose adjoint is not easily derived. Thus, a basic propagation model was developed that captures the AP phenomenon very well. This model is simple and straight forward, providing a basis for deriving the adjoint for the radar data assimilation into WRF.

To assess the ability of the propagation model to model the propagation environment, a case study of a significant AP event of June 7, 2008 in Wilmington, NC was assessed. The model was in good agreement with the observed AP, showing ground reflections at about the same location.

Though the model developed is rapid in terms of numerical processing, the number of points required is daunting. This is due to the step-size of the numerical technique being some percentage of the wavelength. To improve the numerical performance, an optimum wavelength for capturing the fundamental phenomenon was studied. The result was by increasing the wavelength by a factor of 4 reduced the number of grid points by a factor of 16 thereby reducing the CPU time required by a factor of 16.

Future work on the program includes developing the adjoint model to allow the direct ingestion of the radar data and integrate the forward propagator into a WRF module so that WRF may calculate the propagation environment directly.

5. REFERENCES

- Battan, L.J., 1981: **Radar Observation of the Atmosphere**, University of Chicago Press, pp. 324.
- Bean, B.R. and E.J. Dutton, 1966: **Radio Meteorology**, Department of Commerce, pp. 435.
- Bech, J., D. Bebbington, B. Codina, A. Sairouni, and J. Lorente, 1998: Evaluation of atmospheric anomalous propagation conditions: an application for weather radars, *Proceeding of EUROPTO Conference on Remote Sensing for Agriculture, Ecosystems, and Hydrology, Barcelona, Spain, 22 – 24 September*.
- Doviak, R and D. Zrnich, 1993: **Doppler Radar and Weather Observations**, Academic Press, pp. 563.
- Kuttler, J.R. and R. Janaswamy, 2002: Improved Fourier transform methods for solving the parabolic wave equation, *Radio Science*, **37**, 2.
- Leontovich, M. and V. Fock, 1946: Solution of the problem of propagation of electromagnetic waves along the Earth's surface by the method of parabolic equation, *Journal of Physics of the USSR*, **X**, 1, pp. 13-24.
- Levy, M., 2000; **Parabolic Equation Methods for Electromagnetic Wave Propagation**, IET, 336 pp.
- McArthur, R.J. and D. H. O. Bebbington, 1991: Diffraction over simple terrain obstacles by the method of parabolic equations, *Proceedings Seventh International Conference on Antennas and Propagation, 15 – 18 April, York, UK, pp. 824-827*.
- Millington, S. C. Wang, R. Crocker, R. Seaman, W. Lewi, 2007: UK Met Office High Resolution Radar Propagation Project, *Bacimo Conference, 6-8 Nov, Boston, MA*.
- Rinehart, RE., 1991: **Radar for Meteorologists**, Rinehart Publications, pp. 333.
- Sahr, J.D. and F. D. Lind, 1998: Passive radio remote sensing of the atmosphere using transmitters of opportunity, *Radio Science Bulletin*, **284**, p.4-7.
- Stagliano, J, J. C. Kerce, G. M. Hall, R. D. Bock, E. J. Holder, S. F. Dugas, and F. Vandenberghe, 2008: Prediction and Mitigation of Anomalous Propagation with the Total Atmospheric Effects Mitigation (TAEM) System, *24th International Interactive Information and Processing Systems (IIPS) for Meteorology, Oceanography, and Hydrology, 20-24 January New Orleans, LA*.
- Ware, R., P. Herzegh, F. Vandenberghe, J. Vivekanandan, and E. Westwater, 2006: Ground based radiometric profiling during dynamic weather conditions, http://www.radiometrics.com/JAOT_06_preprint.pdf